

Fabrication of superhydrophobic coating with enhanced stability and anti-icing performance

X. Z. Fang^{a,*}, J. W. Shen^b, Z. W. Feng^b, Z. Q. Tang^b

^a *School of Chemistry and Chemical Engineering, Jiangsu University of Technology, Changzhou, 213001, China*

^b *School of Chemistry and Chemical Engineering, Jiangsu University of Technology, Changzhou, 213001, China*

Ice accretion on outdoor equipment detrimentally affect their performance and increase the maintenance cost. Significant advancements have been made in the development of superhydrophobic coatings for anti-icing, however, the intricate manufacturing procedures and limited stability remain primary challenges that hinder their widespread use in practical application. In this context, a durable superhydrophobic coating has been fabricated using a simple spraying technique, achieving a contact angle of $166.7\pm 1.4^\circ$ and a roll-off angle of $0.6\pm 0.2^\circ$. The coating exhibits excellent stability with contact angle maintained above 160° after undergoing various examinations. Meantime, the superhydrophobic coating possesses an enhanced anti-icing property with the time to ice formation prolonged to 42.8 min. This stable superhydrophobic coating, suitable for various outdoor uses, is hoped to contribute to the development of eco-friendly anti-icing coatings.

(Received October 8, 2024; Accepted December 3, 2024)

Keywords: Superhydrophobic, Contact angle, Rolling angle, Stability, Spraying method

1. Introduction

Icing is a natural phenomenon frequently occurred in cold area. The formation of ice sometimes can bring damage to human production and life, such as the traffic accident, power loss of blade airfoil, equipment damage in the aviation, malfunction of electric power transmission, and so on [1-3]. Anti-icing technology has garnered significant interest and many de-icing methods are developed [4-7]. The Active and passive de-icing represent the two primary approaches. The active de-icing methods, such as hot-melt de-icing, mechanical breakage, are simple and effective but restricted in real-world use due to excessive energy expenditure [8-9]. The passive de-icing methods are inspired due to the convenient preparation and lower surface ice adhesion [10]. The passive de-icing method is divided into two categories: lubricated surface and superhydrophobic surface [11-14]. Inspired by the nepenthes, the lubricating coating can significantly weaken the ice adhesion, but easily absorb impurities leading to the invalidation [12]. So, the superhydrophobic surface is

* Corresponding author: 2017500077@jsut.edu.cn
<https://doi.org/10.15251/DJNB.2024.194.1855>

regarded as a highly promising anti-icing solution because of its easy operation and good anti-icing ability [14].

Superhydrophobic phenomenon, inspired by the lotus leaf, have been developed and reported in recent years [15-17]. Featuring a contact angle exceeding 150° and a sliding angle below 10° , the superhydrophobic surface minimizes water droplet adhesion and the area of contact at the interface, which makes it easier for droplets to roll off the surface, thus avoiding the formation of ice and reducing the amount of ice [3]. Various techniques, including electro-spinning, layer-by-layer assembly, electrochemical deposition, spray coating, sol-gel processes, and 3D printing, have been utilized to fabricate superhydrophobic surfaces [18-26]. However, the application of superhydrophobic surfaces is limited due to the weak mechanical stability of their microscopic surface topographies and some complex synthetic process [27-28]. Hence, considering widespread applicability, it is crucial to develop a stable and simple method to obtain the superhydrophobic surface for the de-icing.

In this work, a reliable superhydrophobic coating was produced via an uncomplicated spraying process. With the contact angle of water droplets up to 166.7° and the rolling angle as minimal to 0.6° , the obtained superhydrophobic surface exhibited excellent stability in the adhesion test and the mechanical stability. At the same time, the superhydrophobic surface possessed good anti-icing property with the prolonged icing time and decreased freezing point. Furthermore, the formation of ice on the superhydrophobic surface and the crystallization expansion of water droplets were documented and studied.

2. Experimental

2.1. Materials

All chemical reagents were used as received without further purification. Polyurethane resin (PU), fluorine resin (JF) and fluorine resin (F0) were obtained from Aladdin Chemical Reagent Co., Ltd.. Nano silica and Perfluorooctane triethoxysilane (PFOTES) were purchased from Shanghai Chemical Reagent Co., Ltd.. Deionized (DI) water was obtained from Milli-Q water purification system (resistivity $\sim 18 \text{ M}\Omega \cdot \text{cm}$, Millipore).

2.2. Method for preparing superhydrophobic surface

(1) Preparation of hydrophobic nano-silica

The 1H,1H,2H,2H-perfluoroalkyltriethoxysilanes, ethanol and deionization water were added into a vessel at the ratio of 1:1000:10 by ultra-sonication for 10 min, and then 1g nano-silica was incorporated into the prepared mixture, which was stirred at ambient temperature for 12 h by magnetic stirrers at the rotation speed of $500 \text{ r} \cdot \text{min}^{-1}$. Finally, the stirred solution was filtered, vacuum-dried at 100°C for 3 h to yield the hydrophobic nano silica.

(2) Preparation of spray solution

The polyurethane resin (PU), fluorinated resin (JF) and fluorinated resin (F0) with the weight ratio of 8:5:3 was mixed in acetone. Then the 20 % hydrophobic nano-silica (based on the weight of PU) was incorporated into the acetone solution and stirred at ambient temperature for 3h with a magnetic agitator at the rotational speed of $700 \text{ r} \cdot \text{min}^{-1}$ to disperse evenly in the solution. Finally, the polyurethane and fluorine resin curing agent were added respectively, and continued

stirring for 0.5 h to obtain the prepared spraying solution.

(3) Substrate pretreatment

The aluminum alloy substrate was polished with 1000 mesh sandpaper, and then cleaned with acetone, ethanol and deionized water by ultra-sonication for 5 minutes in order to remove the oil and impurities, and ultimately, it was baked in an oven to be ready for use.

(4) Preparation of the superhydrophobic surface

A 1 mm nozzle spray gun was adopted. With the air pressure of 0.3 MPa and the distance of 20 cm between the nozzle and the substrate, the spray solution was sprayed on the surface of the substrate at a flow rate of 1.3 mL/s, while the moving speed of the spray gun was maintained at 0.2 cm/s. Sprayed again after the first time, more even coating was obtained and then placed in a 100 °C oven for 2 h curing. Finally, the superhydrophobic surface was successfully synthesized.

3. Results and discussion

The polished aluminum alloy was utilized as the hydrophilic surface (named as Al), while the polyurethane superhydrophobic coating was served as the superhydrophobic surface (named as SH coating). Field emission SEM was used to examine the microstructures of the two surfaces: the hydrophilic aluminum alloy surface and the superhydrophobic coated surface. Observed in Figure 1, the aluminum alloy surface, polished using 1000 mesh sandpaper is not entirely smooth and exhibits noticeable striated scratches and a few grooves. At higher magnifications, no nano-scale rough structure can be existed on the surface. Conversely, on the superhydrophobic silica-coated surface, an aggregated micro-nanometer rough structure with numerous tiny pores is observed, which is beneficial for the surface hydrophobicity.

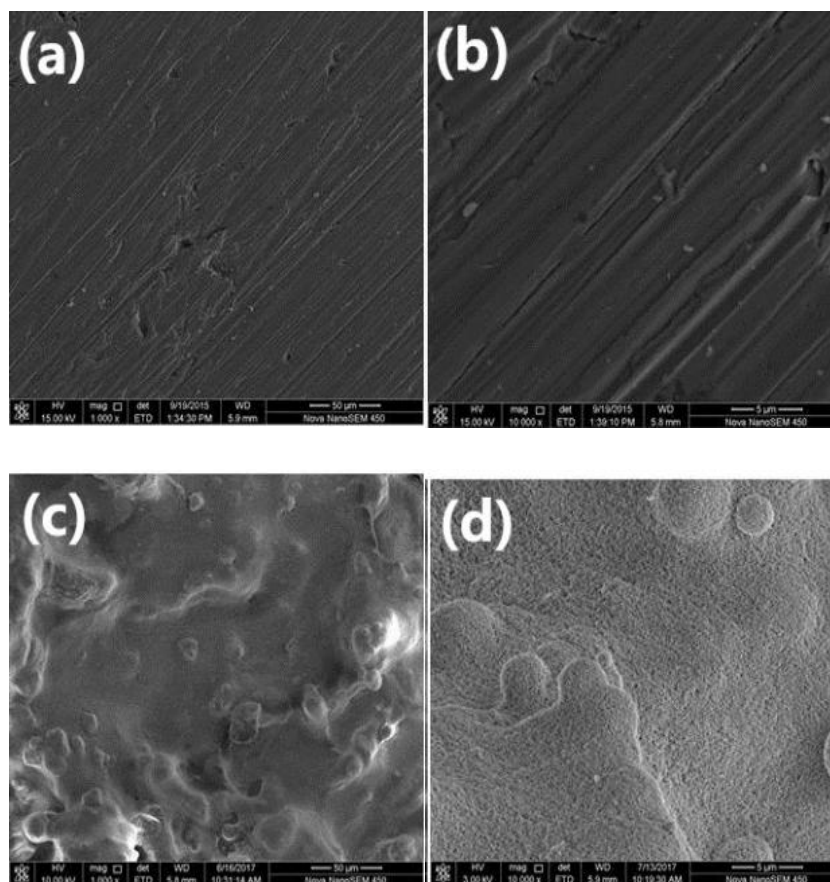


Fig. 1. SEM images of Surface morphology of aluminum alloy (a, b) and superhydrophobic coating (c, d).

The surface wettability was first investigated through the contact angle and rolling angle. As shown in Figure 2, on the Al surface, the water droplets exhibit a contact angle of $53.4 \pm 1.2^\circ$ indicating its hydrophilicity. The water droplets is firmly adhered without slipping off even tilted at a 90° angle. In contrast, on the surface of SH coating, water droplets display a contact angle of $166.7 \pm 1.4^\circ$ with a rolling angle of $0.6 \pm 0.2^\circ$, indicating that the water can rapidly roll off the surface due to the weak adhesion, avoiding the formation of ice.

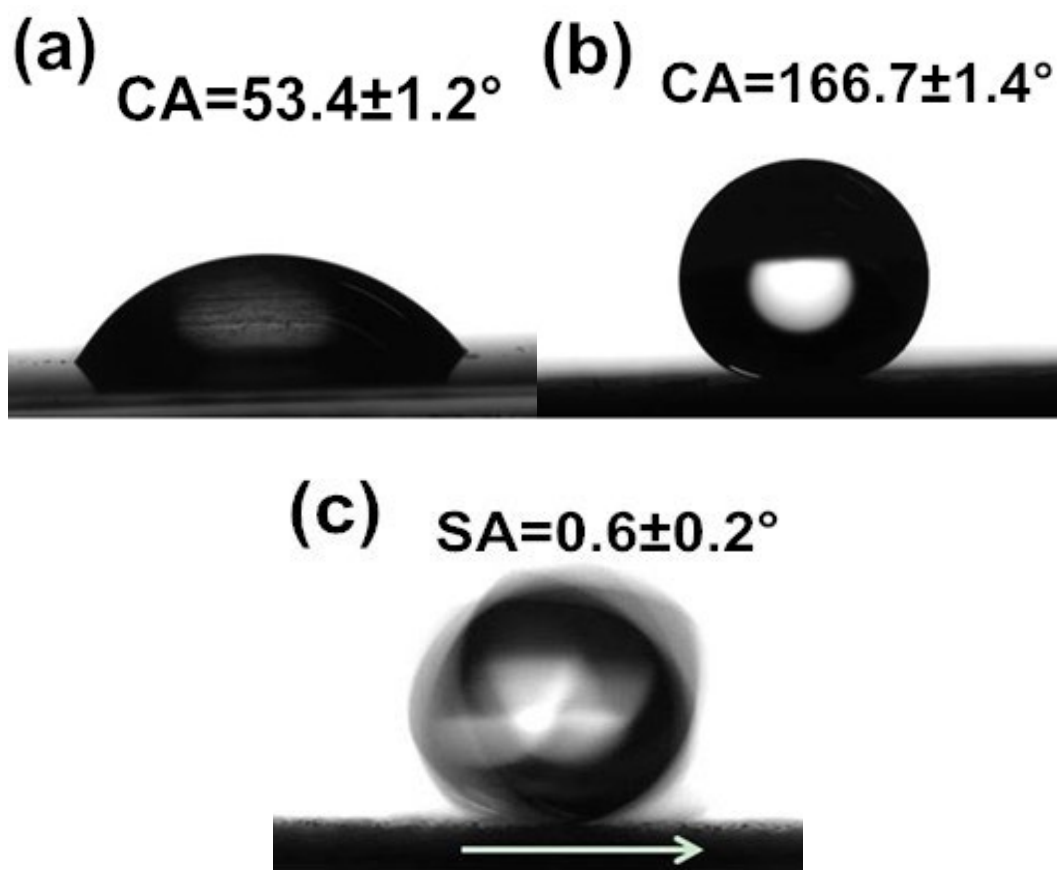


Fig. 2. Photographs of droplet on the surface of Al (a) and SH coating (b, c).

Stability of superhydrophobic surfaces is of importance in practical applications. The adhesion of superhydrophobic coating and the substrate is a key element for the chemical stability. Hence, the adhesion was firstly tested through tape stripping experiments. 3M tape (adhesion value of approximately 0.44 N/mm) with a width of 1.5 cm and a length of 5 cm was applied to the surface of the SH coating. The tape was firmly pressed to ensure close adherence before peeled off. Then the same operation was repeated at the same position with a new piece of tape. The contact angle and rolling angle on the coating surface were recorded with the change of peeling times. As exhibited in Figure 3a, even after 30 repeated stripping experiments, the SH coating maintains the superhydrophobicity with the contact angle of water droplets up to $165.1 \pm 1.8^\circ$ and the rolling angle low to $1.6 \pm 0.3^\circ$, indicating that the SH coating possesses a good adhesion and a good stability. In addition, the durability of the superhydrophobic surface is crucial. In application, the coating structure with low surface energy and the micro-roughness can be destroyed by physical damage.

So that, the next tests were performed assess the structural durability through using the atomized water flow to rinse the surface at different speeds and durations. As exhibited in Figure 3b, the superhydrophobic coating was impact by the atomized water droplets with various speed for 30 seconds. It is evident that when atomized water impacts the surface at speeds ranging from 0 to 50 m/s, the contact angle and rolling angle of water droplets on the SH coating remain largely unchanged, indicating a good stability is existed under this condition. At the same time, controlling the flow speed at 50 m/s, the SH coating was impacted under atomized water droplets with different times. As depicted in Figure 3c, the contact angle of water droplets on the SH coating tends to diminish as the impact time increases, while the rolling angle of water droplets gradually increases. This can be explained that under the test condition, some surface hydrophobic nano-silica particles can be shed, causing small damage to the microscopic rough structure. However, even though impacted for 60 min under high-speed water flow, the SH coating still has the superhydrophobic property with the contact angle of $161.3 \pm 2.2^\circ$ and the rolling angle of $8.6 \pm 0.8^\circ$, indicating that the SH coating exhibits good impact resistance stability due to the strong chemical adhesion.

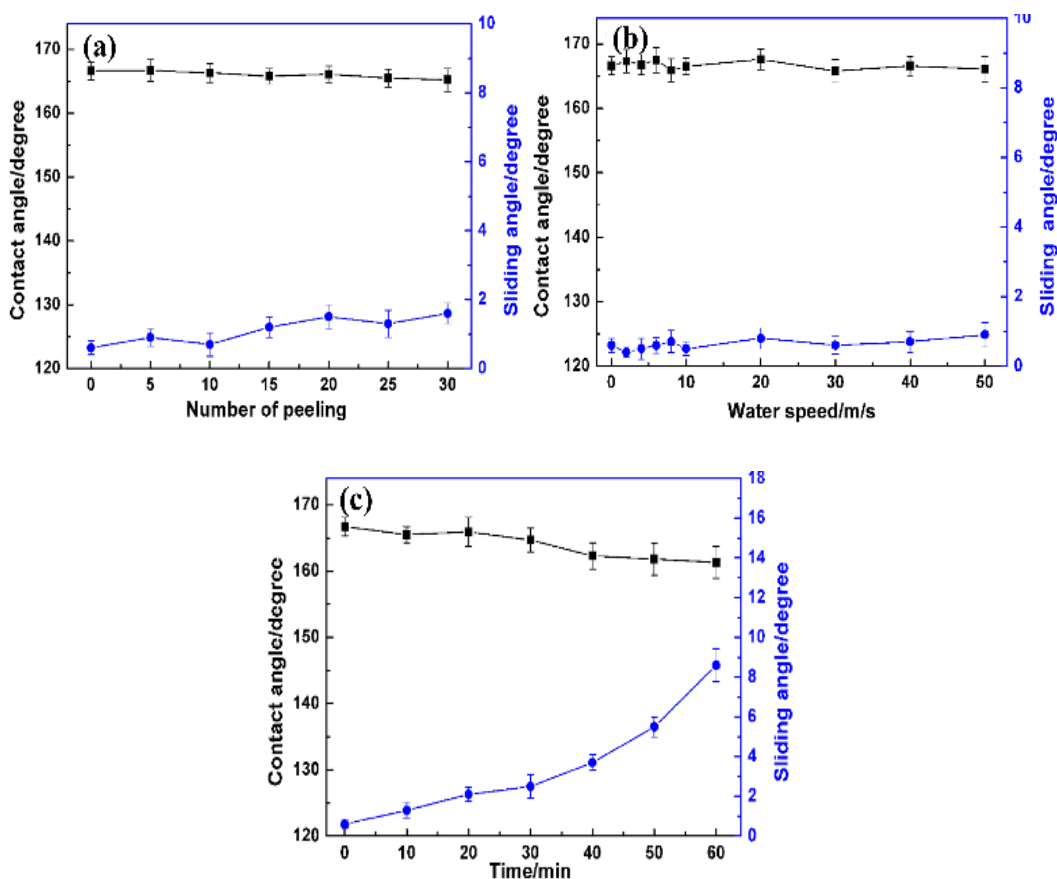


Fig. 3. The variation of contact angle and the rolling angle for water dropletson the SH coating after (a) adhesion tests, (b) water impact tests with different speed and (c) water impact tests with different time.

The anti-icing performance of samples were investigated by after establishing the stability. In Figure 4a, the ice formation delay tests were investigated with the temperature set to -10°C and the relative humidity set to $67 \pm 0.5\%$. It can be clearly observed that undergoing three stages of

cooling, freezing nucleation and freezing growth during the complete freezing process, the water droplets on SH coating begin to freeze at 180.4 s and turn completely from liquid to solid at 210.3 s to form peach shaped ice. As a reference, the water droplets on Al surface begin to freeze at 33.2 s and completely ice at 36.1 s. Compared with the icing delay behavior on aluminum alloy, the superhydrophobic surface delayed the freezing of water droplets by 147.2 seconds, and the time to completely freeze is about 6 times than that of the Al surface. At the same time, the time delay until water droplets freeze at various temperatures were also tested. As shown in Figure 4b, with the relative humidity at $73 \pm 0.8\%$, the freezing time of water droplets on aluminum alloy and superhydrophobic surfaces decreases with the decrease of temperature. When the cold surface is $-4\text{ }^{\circ}\text{C}$, droplets of water on the Al surface freeze completely in 63 s, while droplets of water on the SH coating surface freeze after 42.8 minutes, exhibiting a good anti-icing property. As the temperature low to $-15\text{ }^{\circ}\text{C}$, it takes 7 s and 62 s to completely freeze for water on the surface of Al and SH coating, respectively. The anti-icing effect of the SH coating weakens with decreasing temperature.

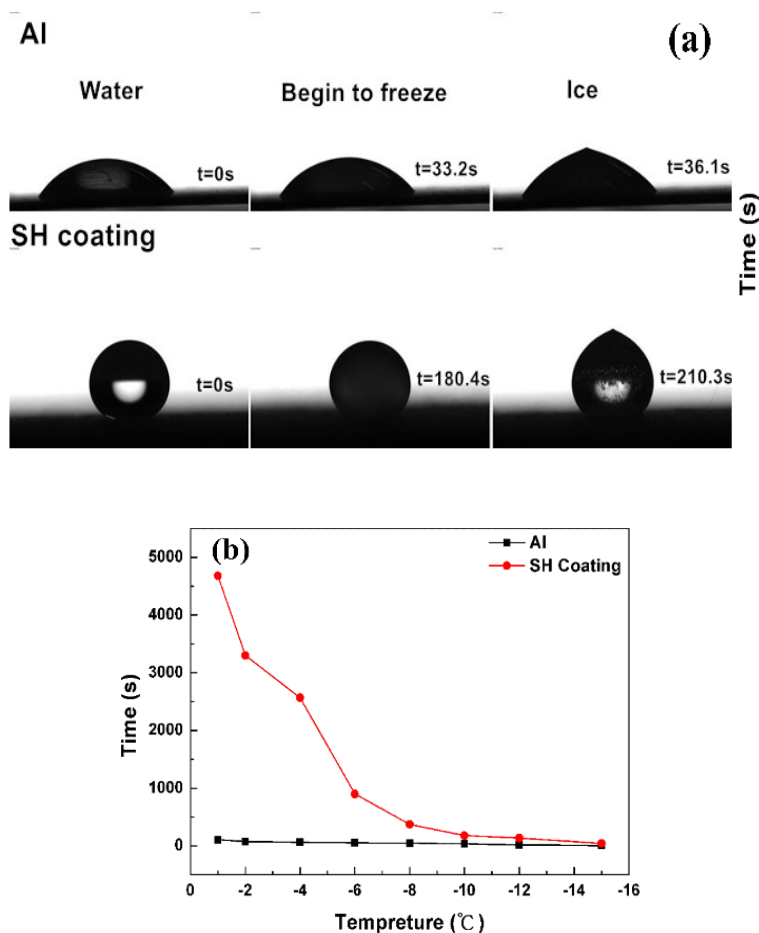


Fig. 4. (a) The icing delay behavior for water droplets under $-10\text{ }^{\circ}\text{C}$. (b) The icing delay time for water droplets at different temperature.

In order to explain this phenomenon, the changes of water droplet contact angles during the cooling process were investigated. As observed in Figure 5, the initial contact angle of water droplets on the Al surface is 53.7° , which only decreases by 0.3° to 53.4° when the water completely freeze

at 33.1 s. In contrast, on the SH coating surface, the initial contact angle is 165.8° and rapidly decreases to 149.3° after 168.5 s. On the superhydrophobic surface, the water droplets exist with a significant amount of air trapped within the grooves and holes of the micro-rough structure. During the cooling process, the air undergoes expansion and contraction, leading to some water droplets penetrating into the grooves. Simultaneously, water vapor in the groove condenses into small droplets contacted with larger water droplets on the surface, enhancing their adsorption performance on the surface. Furthermore, as the surface temperature decreases, there is an increase in material surface tension due to the weakened molecules thermal movement, leading to enhanced adsorption of water droplets onto the surfaces. Thus, as the contact angles decrease with the temperature, the interaction between water and interface increases, which lead to an increase in ice nucleation rate and accelerated nucleus growth rate.

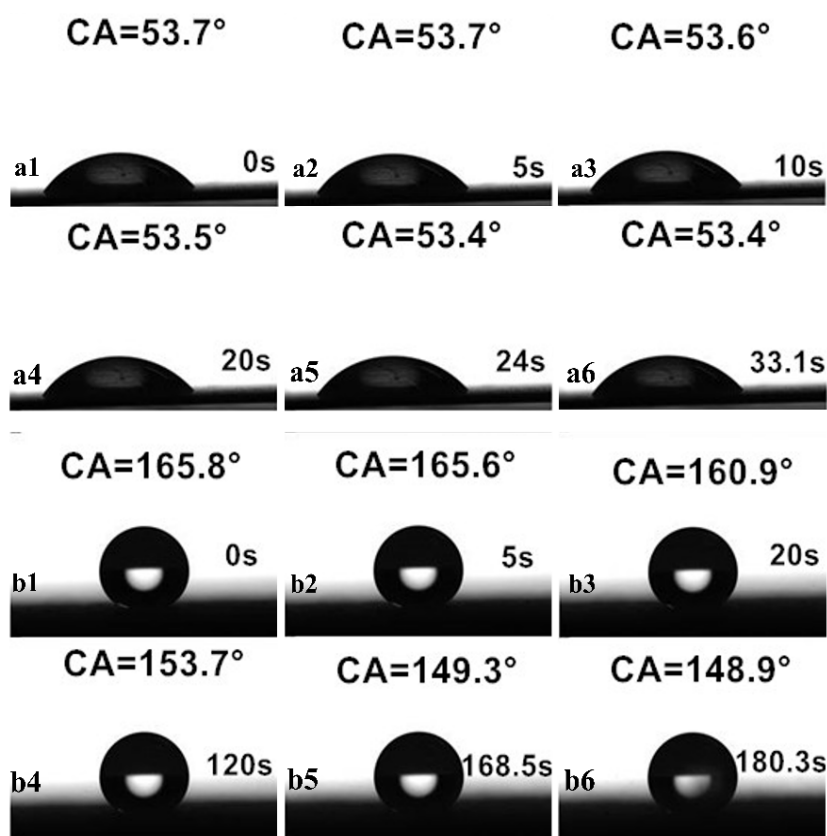


Fig. 5. The change of contact angles during the cooling process for water droplets on the surface of (a) Al and (b) SH coating.

In conclusion, the superhydrophobic coating was successfully fabricated through a simple spraying method on the Al substrate. Due to the strong adhesion and good impact resistance, the as-prepared SH coating with a contact angle of $166.7 \pm 1.4^\circ$ and a rolling angle of $0.6 \pm 0.2^\circ$, exhibits a good stability in the tests. At the same time, the SH coating shows an enhanced anti-icing property with the icing delay time 6 times than that on the Al surface. This work will provide a simple method to construction a stable anti-icing coatings and make them more suitable for the outdoor application.

Author contributions

All author contributions equally in this work.

Conflicts of interest

There are no conflicts to declare.

Acknowledgements

This work is supported by the National Natural Science Foundation of China (No. 52073127) and the Natural Science Foundation of Department of Science and Technology of Jiangsu Province (No. BK20191034).

References

- [1] L. Wang, Z. Tian, G. Jiang, X. Luo, C. Chen, X. Hu, H. Zhang, M. Zhong, *Nature Commun.*, 13 (2020) 378
- [2] S. Xu, Z. Zhou, L. Feng, N. Cui, N. Xie, *Processes*, 9 (2021) 291; <https://doi.org/10.3390/pr9020291>
- [3] Y. Li, A. Sha, Z. Tian, Y. Cao, X. Li, Z. Liu, *J. Mater. Sci.*, 58 (2023) 3377-3400; <https://doi.org/10.1007/s10853-023-08212-0>
- [4] S. Jiang, Y. Diao, H. Yang, *Adv. Colloid Interface Sci.*, 308 (2022) 102756; <https://doi.org/10.1016/j.cis.2022.102756>
- [5] T. Wang, Y. Zheng, A.-R. O. Raji, Y. Li, W. K. A. Sikkema, J. M. Tour, *ACS Appl. Mater. Interfaces*, 8 (2016) 14169-14173; <https://doi.org/10.1021/acsami.6b03060>
- [6] J. Wei, S. Yang, X. Xiao, J. Wang, *Langmuir*, 40 (2024) 7747-7759; <https://doi.org/10.1021/acs.langmuir.4c00440>
- [7] Z. Xie, H. Wang, Y. Geng, M. Li, Q. Deng, Y. Tian, R. Chen, X. Zhu, Q. Liao, *ACS Appl. Mater. Interfaces*, 13 (2021) 48308-48321; <https://doi.org/10.1021/acsami.1c15028>
- [8] Z. He, H. Xie, M. I. Jamil, T. Li, Q. Zhang, *Adv. Mater. Interfaces*, 9 (2022) 2200275; <https://doi.org/10.1002/admi.202200275>
- [9] Y. Meng, Y. Li, J. Chen, Z. Wang, J. Lai, C. Zhang, F. Meng, P. Chen, *Constr. Build. Mater.*, 425 (2024) 135883; <https://doi.org/10.1016/j.conbuildmat.2024.135883>
- [10] X. Huang, N. Tepylo, V. Pommier-Budinger, M. Budinger, E. Bonaccorso, P. Villedieu, L. Bennani, *Prog. Aeosp. Sci.*, 105 (2019) 74; <https://doi.org/10.1016/j.paerosci.2019.01.002>
- [11] C. Wang, Z. Guo, *Nanoscale*, 12 (2020) 22398-22424; <https://doi.org/10.1039/D0NR06009G>
- [12] L. B. Boinovich, K. A. Emelyanenko, A. M. Emelyanenko, *J Colloid Interface Sci.*, 606 (2022) 556-566; <https://doi.org/10.1016/j.jcis.2021.08.030>

- [13] Y. Xia, W. Gu, L. Shao, X. Jiao, Y. Ji, W. Deng, X. Yu, Y. Zhang, Y. Zhang, *Chem. Eng. J.*, 476 (2023) 146746; <https://doi.org/10.1016/j.cej.2023.146746>
- [14] L. Wang, Q. Gong, S. Zhan, L. Jiang, Y. Zheng, *Adv. Mater.*, 28 (2016) 7729-7735; <https://doi.org/10.1002/adma.201602480>
- [15] S. G. Moghadam, H. Parsimehr, A. Ehsani, *Adv. Colloid Interface Sci.*, 290 (2021) 102397; <https://doi.org/10.1016/j.cis.2021.102397>
- [16] N. J. Shirtcliffe, G. McHale, S. Atherton, M. I. Newton, *Adv. Colloid Interface Sci.*, 161 (2010) 124-138; <https://doi.org/10.1016/j.cis.2009.11.001>
- [17] W. Zhang, D. Wang, Z. Sun, J. Song, X. Deng, *Chem. Soc. Rev.*, 50 (2021) 4031-4061; <https://doi.org/10.1039/D0CS00751J>
- [18] Y. Bao, Y. Zhang, J. Ma, *Nanoscale*, 12 (2020) 16443-16450; <https://doi.org/10.1039/D0NR02571B>
- [19] D. Ning, Z. Lu, C. Tian, N. Yan, L. Hua, *Sep. Purif. Technol.*, 342 (2024) 127052; <https://doi.org/10.1016/j.seppur.2024.127052>
- [20] W. Gu, W. Li, Y. Zhang, Y. Xia, Q. Wang, W. Wang, P. Liu, X. Yu, H. He, C. Liang, Y. Ban, C. Mi, S. Yang, W. Liu, M. Cui, X. Deng, Z. Wang, Y. Zhang, *Nature Commun.*, 14 (2023) 5953; <https://doi.org/10.1038/s41467-023-41675-y>
- [21] R. Wang, X. Zhao, Y. Lan, L. Liu, C. Gao, *J. Membr. Sci.*, 615 (2020) 118566; <https://doi.org/10.1016/j.memsci.2020.118566>
- [22] S. Yuan, C. Chen, A. Raza, R. Song, T.-J. Zhang, S. O. Pehkonen, B. Liang, *Chem. Eng. J.*, 328 (2017) 497-510; <https://doi.org/10.1016/j.cej.2017.07.075>
- [23] P. Liu, S. Liu, X. Yu, Y. Zhang, *Chem. Eng. J.*, 406 (2021), 127153; <https://doi.org/10.1016/j.cej.2020.127153>
- [24] D. Aslanidou, I. Karapanagiotis, C. Panayiotou, *Prog. Org. Coat.*, 97 (2016) 44-52; <https://doi.org/10.1016/j.porgcoat.2016.03.013>
- [25] Z. Xiao, L. Zhang, W. Zhang, X. Yu, Y. Zhang, *J. Bionic. Eng.*, 15 (2018) 1025-1034; <https://doi.org/10.1007/s42235-018-0090-0>
- [26] W. Deng, Y. Liu, Y. Rui, G. Lu, J. Liu, *Prog. Org. Coat.*, 181 (2023) 107570; <https://doi.org/10.1016/j.porgcoat.2023.107570>
- [27] S.P. Dalawai, M. A. S. Aly, S. S. Latthe, R. Xing, R. S. Sutar, S. Nagappan, C.-S. Ha, K. K. Sadasivuni, S. Liu, *Prog. Org. Coat.*, 138 (2020) 105381; <https://doi.org/10.1016/j.porgcoat.2019.105381>
- [28] D. Zhang, L. Li, Y. Wu, B. Zhu, H. Song, *Appl. Surf. Sci.*, 473 (2019) 493-499; <https://doi.org/10.1016/j.apsusc.2018.12.174>